Ball-milling-induced amorphization in Ni_xZr_y compounds: A parametric study

Y. Chen, M. Bibole, R. Le Hazif, and G. Martin
Centre d'Etudes de Saclay, Centre de Recherches sur les Matériaux,
Section de Recherches de Métallurgie Physique, 91191 Gif-sur-Yvette CEDEX, France
(Received 7 January 1993)

A vibrating frame grinder has been instrumented for evaluating the amplitude and frequency of ball oscillation, as a function of the amplitude of vibration of the frame and of the ball mass. Based on such measurements, it is found that Ni_xZr_y compounds become fully amorphized provided the specific milling intensity is greater than a temperature- and composition-dependent threshold value. The specific milling intensity is the momentum transferred by the ball to the unit mass of powder per unit time. Below this threshold, a two-phase structure (crystalline+amorphous) is stabilized; the steady proportion of the amorphous phase increases with the milling intensity and decreases on increasing the milling temperature. The intensity threshold increases with temperature and varies in the opposite direction as the hardness of the starting crystalline compound. The amorphous NiZr phase can be obtained by two distinct routes, either starting from the crystalline compound NiZr, or from a mixture of $Ni_{10}Zr_7$ and $NiZr_2$ amorphous phases. These routes correspond, respectively, to an increase and a decrease in internal energy.

I. INTRODUCTION

High-energy ball milling is currently used for stabilizing nonequilibrium phases: solid-state amorphization is a well-documented example. As can be seen from early literature data,[1] full amorphization depends, in a yet obscure way, on the milling conditions and device. As an example, improved amorphization of Ni_xTi_{1-x} in a Spex 8000 mill was reported when milling is performed at low temperature (-35 °C).[2] It is often claimed that milling-induced phase transitions result from the accumulation of defects in the mother phase: an increase of the (internal or free) energy would result in the loss of stability. Milling conditions would adjust the rate and level of defect accumulation. As discussed elsewhere,[3] such an argument lacks theoretical basis (why should the parent phase store more energy than the daughter phase?) and an alternative way of looking to milling-induced phase transitions has been proposed. Under milling conditions, the surrounding of an atom changes in time because of two mechanisms acting in parallel: thermally activated jumps of point defects, as under classical thermodynamic equilibrium conditions, and forced processes such as shearing, sticking of powders along freshly formed surfaces, etc. When such is the case, a theoretical framework exists[4] which shows that the respective stability of various phases can be predicted from a stochastic potential; the latter can be computed (in simple cases) from microscopic data such as pair interaction energies, atomic jump frequencies, etc. The stability field of various phases is then better described in a generalized phase diagram: temperature vs composition vs "forcing parameter." The forcing parameter is shown to be the ratio of the forced atomic jump frequency to the thermally activated one.

In the last couple of years, a few experiments have indeed shown that full amorphization can only be obtained for a well-defined range of milling conditions for a given mill.[5–7] Eckert, Schultz, and Urban[7] have investigated qualitatively the influence of milling intensity on the glass formation of Ni_xZr_{1-x} mixtures in a planetary mill. The ball milling was performed with the intensity setting 3, 5, or 7 corresponding to a calculated velocity of the ball respectively equal to 2.5, 3.6, or 4.7 ms^{-1} (or to a kinetic energy of 14, 29, or 49 mJ for each ball). The x-ray-diffraction patterns of several Ni_xZr_{1-x} samples after 60 h of mechanical alloying at milling intensities 3, 5, and 7, demonstrated that concentration ranges for full amorphization are different for the three intensities. In other words, using different intensities results in different end products for the same concentration (fully amorphous or a mixture of crystalline and amorphous phases).

A more quantitative investigation was presented by Gaffet *et al.*[5–6] using a modified planetary mill which allows independent variation of the (clockwise) rotation rate, Ω, of the disc on which the vial holders are fixed, and of the (counterclockwise) rotation rate, ω, of the vial. As a first guess, the energy of the balls in the vial is roughly proportional to Ω^2, while the frequency of collision of the balls with the vial increases with ω. The latter two quantities can thus be varied independently. An Ω vs ω window is identified, within which the end product after 40–48 h milling is a homogeneous amorphous phase. Outside this domain, a mixture of amorphous and crystalline phases is observed. Gaffet also compared the Ω vs ω windows for full amorphization in two mills with a different disc radius R. The two windows overlap provided Ω^2R (i.e., the energy of the balls) is kept the same.

However, the planetary mills used in these experiments do not allow for a safe estimate of the characteristics of the impact as a function of the milling conditions. It is the reason why we have built a very simple device which allows for a reasonable estimate thereof, and performed a systematic study of the conditions for full amorphization of model compounds (Ni_xZr_y) in this device.

II. EXPERIMENTAL SETUP AND PROCEDURE

A vibrating frame grinder "Pulverisette O (Fritsch)" has been used. The vial has been modified as shown in Fig. 1. It consists of a tungsten carbide bowl (ϕ 95 mm), the temperature of which can be regulated in the range $-190-+250$ °C by circulating a fluid with controlled temperature in a jacket. Milling at 200 °C could be performed during several hundred hours. The milling temperature is monitored by a thermocouple inserted into the bottom of the WC vial. A hardened steel ball with a mass in the range 0.1–1.0 kg is used. For preventing oxidation or nitridation of the powder during milling, a vacuum tight cover was designed: a good seal is obtained with a Teflon O ring for the room- and high-temperature runs; a metallic seal was used for the low-temperature ones. The vial can be evacuated (10^{-5} Torr) prior to milling, owing to the value shown in Fig. 1.

Depending on the vibration amplitude of the frame, the mass of the ball and the quantity of metallic powder in the vial, the ball achieves an up and down movement, the frequency of which is depicted in Table I. The data of Table I were obtained from a linear variable differential transducer attached to the top of the vial as shown in Fig. 1.

The description of the movement of the ball in the vial is of prime importance for this study. It is easily checked that in the absence of powder in the vial, the collision of the ball is mostly elastic: this is easily checked by dropping the ball from ≈ 1 to 2 cm above the empty immobile vial and listening for at least one bounce. Also when the vibrating frame is turned on in the absence of powder, the jump height of the ball is very irregular and may suddenly become very large, as expected for collisions with a restitution coefficient of 1.[8,9] With powder in the vial, on the opposite, the collision is purely plastic: performing the same test as above, a single collision will be heard, after the collision, the velocity of the ball with respect to the powder is zero. When the vibrating frame is turned on, in the presence of powder in the vial, the ball achieves an almost periodic up and down movement, as detected by the LVDT attached to the cover of the vial. Figure 2 gives typical records of such a movement for three different vibration amplitudes of the frame. The jump height of the ball cannot be trusted because of uncon-

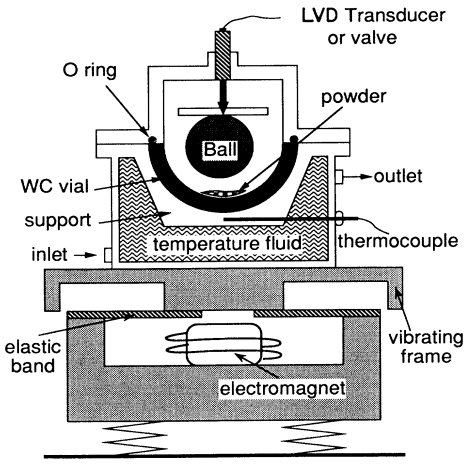

FIG. 1. Scheme of the modified vibrating frame milling device.

TABLE I. Summary of the milling experiments performed on Ni_xZr_y alloys. N is the label of the run. M_b is the mass of the ball (measured). A is the vibration amplitude of the vial (measured). f is the impact frequency of the ball with the powder in the vial (measured). V_{max} is the maximum velocity of vial ($=A\omega$); $\approx$average velocity of the ball relative to the vial at the time of collision ("cf." the Appendix I). M_p is the mass of powder in the vial. EP is the end product (a, amorphous phase; $a+c$, amorphous+crystalline phases). T is the milling temperature. t is the duration of milling.

N	Ni_xZr_y	M_b (kg)	A (mm)	f (Hz)	$\frac{M_b V_{max} f}{M_p}$ (10^3 ms^{-2})	T (°C)	t (h)	
1	$Ni_{10}Zr_7$	1.00	1.5	23	2.17	20	90	a
2	$Ni_{10}Zr_7$	1.00	1.0	30	1.88	20	104	a
3	$Ni_{10}Zr_7$	1.00	0.5	33	1.04	20	98	a
4	$Ni_{10}Zr_7$	0.50	1.5	20.	0.94	20	95	a
5	$Ni_{10}Zr_7$	0.50	1.0	25	0.79	20	114	a
6	$Ni_{10}Zr_7$	0.50	0.5	35	0.55	20	137	a
7	$Ni_{10}Zr_7$	0.30	1.5	19	0.54	20	118	a
8	$Ni_{10}Zr_7$	0.30	1.2	21	0.48	20	256	$a+c$
9	$Ni_{10}Zr_7$	0.30	1.0	23	0.43	20	380	$a+c$
10	$Ni_{10}Zr_7$	0.30	0.5	35	0.33	20	123	$a+c$
11	$Ni_{10}Zr_7$	0.175	1.0	25	0.41	20	228	$a+c$
12	$Ni_{10}Zr_7$	0.11	1.5	25	0.26	20	267	$a+c$
13	$Ni_{10}Zr_7$	0.11	1.0	30	0.21	20	325	$a+c$
14	NiZr	1.00	1.0	30	1.88	20	153	a
15	NiZr	1.00	0.5	33	1.04	20	190	a
16	NiZr	0.50	1.5	20	0.94	20	94	a
17	NiZr	0.50	1.0	25	0.79	20	173	$a+c$
18	NiZr	0.30	1.5	19	0.54	20	259	$a+c$
19	$NiZr_2$	1.00	1.5	23	2.17	20	142	a
20	$NiZr_2$	1.00	1.0	30	1.88	20	138	a
21	$NiZr_2$	0.50	1.5	20	0.94	20	245	$a+c$
22	$NiZr_2$	0.50	1.0	25	0.79	20	274	$a+c$
23	Ni_5Zr_2	0.50	1.0	25	0.79	20	200	a
24	Ni_5Zr_2	0.30	1.0	23	0.43	20	238	$a+c$
25	Ni_5Zr eutectic	0.50	1.5	20	0.94	20	90	$a+c$
26	63.5% at. Zr eutectic	0.50	1.5	20	0.94	20	133	a
27	63.5% at. Zr eutectic	0.30	1.0	23	0.43	20	255	a
28	63.5% at. Zr	0.175	1.5	25	0.41	20	286	$a+c$
29	54.4% at. Zr	0.50	1.5	20	0.94	20	185	a
30	54.4% at. Zr	0.30	1.5	19	0.54	20	264	$a+c$
31	54.4% at. Zr	0.30	1.0	23	0.43	20	266	$a+c$
32	$Ni_{10}Zr_7$	0.50	1.5	20	0.94	200	247	a
33	$Ni_{10}Zr_7$	0.50	0.5	35	0.55	200	330	$a+c$
34	$Ni_{10}Zr_7$	0.30	1.0	23	0.43	200	329	$a+c$
35	$Ni_{10}Zr_7$	0.50	0.5	35	0.55	−183	70	$a+c$

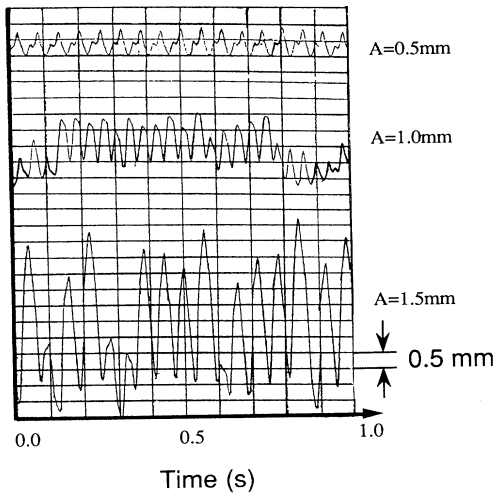

FIG. 2. Typical records of the movement of the ball relative to the vial, as given by the LVDT, for vibration amplitudes of the vial: $A=0.5$, 1.0, and 1.5 mm, respectively.

trolled inertial effects in the LVDT; the frequency of collisions between the ball and the powder is however, quite reliable. It is no surprise that the movement is almost periodic: after each collision, the ball comes to rest with respect to the powder until the frame reaches again the critical velocity for the ejection of the ball. Irregularities in the movement of the ball result from collisions of the ball with larger harder grains in the powder: such collisions bounce the ball laterally. As discussed in the Appendix, for the device we used the critical velocity for the ejection of the ball is very close to the maximum velocity of the frame, $V_{\max} \approx A\omega$, with A the amplitude and f ($\omega=2\pi f$) the frequency of vibration of the vial. As a first approximation, it can be assumed that the collision occurs at any time in the vibration period of the frame: for a large number of collisions, the average momentum transfer to the powder is $M_b V_{\max}$.

Precursor alloys are prepared by levitation melting small quantities (≤ 20 g) of high-purity Ni and Zr; 5 g of the intermetallic compound are introduced into the vial which is then sealed and evacuated. Milling is performed in static vacuum. In the course of milling, small quantities of powder are periodically taken out of vial for structural and microstructural characterization: this is done in a glove box under argon atmosphere. The vial is then resealed, reevacuated, and the milling run is continued.

The morphology of the powder is studied by scanning electron microscopy. The microstructure of the grains forming the agglomerates is studied by transmission electron microscopy: thin samples (with 60–80 nm thickness) are microtomed from powder agglomerates consolidated by epoxy. The crysallographic structure of the phases formed in the powder is determined from x-ray powder diffraction spectra. X-ray-diffraction spectra are deconvoluted numerically with the aid of the algorithm ABFFIT.[10] The spectrum is modeled as a polynomial background plus a set of Gaussian peaks. After some milling time, a broad peak superimposes to the crystalline distorted peaks: the former is interpreted as the contribution of an amorphous phase, the presence of which is confirmed by transmission electron microscopy (TEM) observations: the fraction of the amorphous phase is roughly estimated by the ratio of the integrated diffraction intensity of the broad peak to the total diffracted intensity (Ia/Is). This procedure has been calibrated on "handmade" mixtures of crystalline and amorphous powders in various proportions: the correlation is excellent in the range 20–90 % but with a systematic 5% underestimate of the real value. Full experimental details are given in Ref. 8.

III. EXPERIMENTAL RESULTS

The most detailed studies have been performed at room temperature on the $Ni_{10}Zr_7$ compound. They allow one to identify the physical ingredients of the *milling intensity* which controls the nature of the end product. Temperature and composition effects have also been studied on a broad variety of NiZr compounds.

A. Identification of a milling intensity

Figure 3 is a typical sequence of x-ray-diffraction patterns obtained from the intermetallic compound $Ni_{10}Zr_7$ after increasing milling times; the ball used in this run has a mass of 500 g and the vibration amplitude of the frame is 1.5 mm. Full amorphization is obtained beyond 95 hs. The transformation path from the initial crystalline phase to the final amorphous phase is revealed by TEM. The dark-field images of Fig. 4 show that crystalline particles are surrounded by an amorphous cement: on increasing the milling time, the amorphous matrix dissolves the crystallites until full amorphization. The corresponding electron-diffraction patterns are given in Fig. 5. The important feature to note is that the two phases coexist in each powder grain.

Under certain milling conditions, full amorphization cannot be obtained, even for very long milling times. For

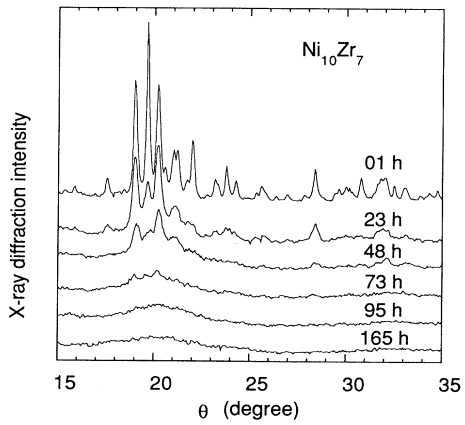

FIG. 3. X-ray-diffraction patterns of $Ni_{10}Zr_7$ after increasing milling times at room temperature, with a ball mass of 0.5 kg, and a vibration amplitude of 1.5 mm. A fully amorphous phase is obtained beyond 95 h.

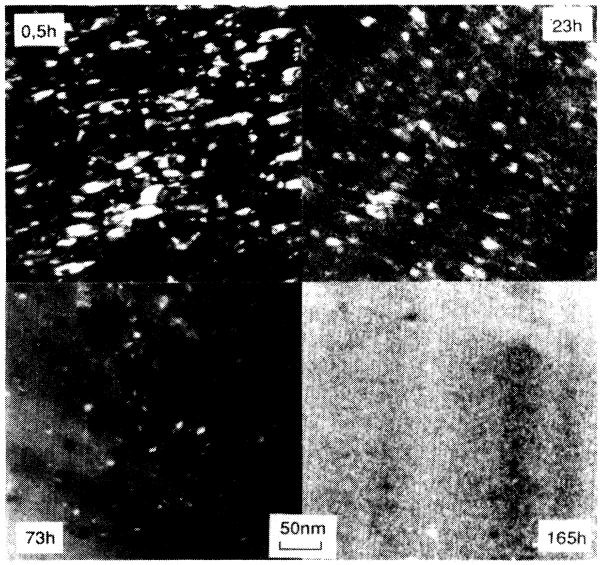

FIG. 4. Dark-field TEM micrographs of $Ni_{10}Zr_7$ milled for 0.5, 23, 73, and 165 h at room temperature with a ball mass of 0.5 kg and a vibration amplitude of 1.5 mm.

example, with a ball of 300 g and a vibration amplitude of 1.0 mm, some crystalline diffraction peaks can still be identified after 370 h (Fig. 6). A two-phase mixture is observed by TEM (Fig. 7). As above, nanometer-sized crystallites are dispersed in the amorphous phase.

Such experiments have been carried out with a large variety of vibration amplitudes and ball masses for different alloy compositions. The results are summarized in Table I. Figure 8 shows typical evolutions of the fraction of amorphized compound in $Ni_{10}Zr_7$ as a function of milling time. Two distinct typical behaviors are to be noticed: With milling conditions denoted 4, the fraction of

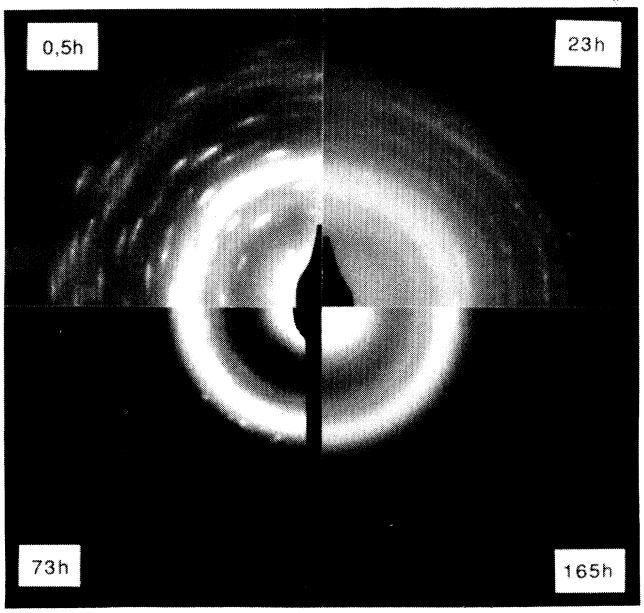

FIG. 5. Corresponding electron-diffraction patterns.

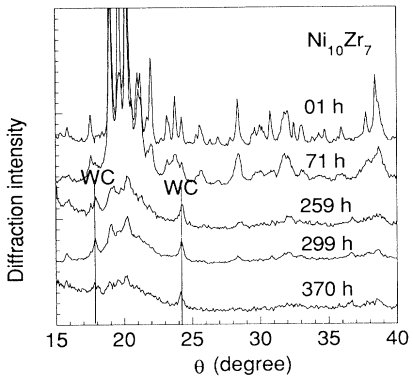

FIG. 6. X-ray-diffraction patterns of $Ni_{10}Zr_7$ milled at room temperature with a ball mass of 0.3 kg and a vibration amplitude of 1.0 mm. Notice the crystalline phase is still detected after 370-h milling.

amorphized compound increases rapidly up to 100%. Full amorphization is achieved under such milling conditions. With milling conditions denoted 9 and 13, the fraction of amorphous phase increases slowly and then saturates to a constant level. Notice the long durations of milling which have been used in order to make sure that a true steady state is achieved. Two-phase equilibrium is achieved under such milling conditions.

The type of end product of all runs performed at room temperature on the $Ni_{10}Zr_7$ compound is presented in Fig. 9 as a function of milling conditions: each experiment is referenced by an impact momentum ($M_b V_{max}$) and an impact frequency. Notice that the impact

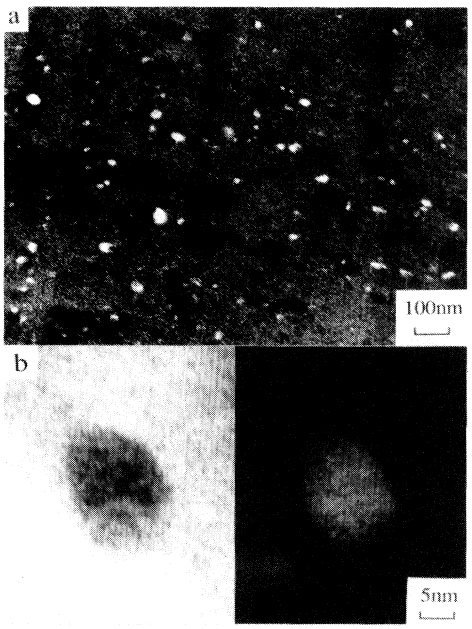

FIG. 7. (a) Dark-field micrograph of $Ni_{10}Zr_7$ milled for 370 h with a ball mass of 300 g and a vibration amplitude of 1.0 mm. (b) High magnification bright and dark-field images of a nanometer size crystallite surrounded by the amorphous phase. Notice the high quality of the crystalline phase where the lattice planes seem undistorted.

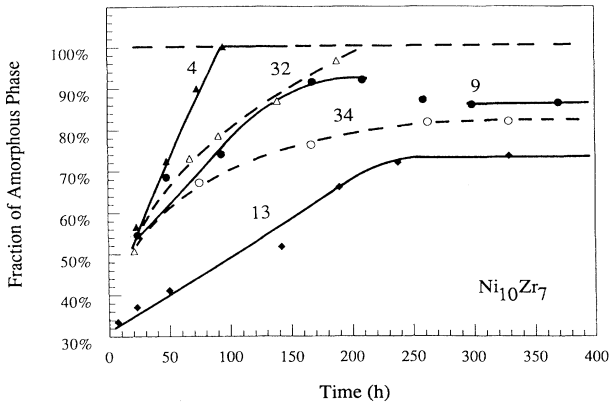

FIG. 8. Fraction of amorphous phase in $Ni_{10}Zr_7$ as a function of milling time for various milling conditions: room temperature (bold symbols, solid line) or 200 °C (open symbols, dashed line). The label refers to Table I. Notice the bold circles represent two distinct experiments: one up to 200 h with four interruptions for picking up powder for x-ray characterization, the second one with an initial milling period of 260 h followed by two more periods up to 380 h. The steady-state fraction of the amorphous phase in both experiments is slightly different.

momentum ($M_b V_{max}$) and frequency f are plotted on a log scale, so that milling treatments with the same value of $M_b V_{max} f$ fall on a straight line with slope -1. As can be seen, full amorphization is obtained provided $M_b V_{max} f$ is larger than a minimum value: below this value, a two-phase structure is stabilized. In other words, the same end product can be obtained by either transferring a large impact momentum at a small frequency or a smaller momentum at a higher frequency (e.g., compare runs 6 and 7). Plotting the results according to other combinations of the milling parameters (e.g., impact energy and frequency) did not give as clear a border between the two types of end products.[8]

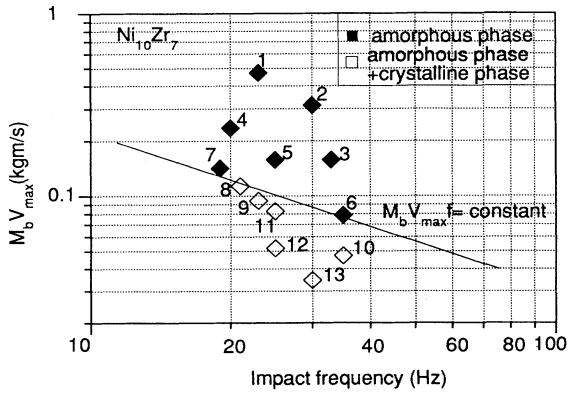

FIG. 9. Steady-state structure of $Ni_{10}Zr_7$ as a function of milling conditions as defined by the momentum transfer at the impact and the impact frequency: bold squares represent the amorphous phase, open squares represent the mixture of amorphous and crystalline phases. The boundary between the two types of steady-state structures fits well with a line of constant value for $M_b V_{max} f$.

We therefore propose to define the milling conditions in our device by a "specific milling intensity" defined as

$$I^* = \frac{M_b V_{max} f}{M_p} ,$$

where M_b is the mass of the ball, V_{max} the maximum velocity of the frame, f the impact frequency, and M_p the mass of powder in the vial. Indeed, the milling intensity can be normalized to the mass of powder, since the impact frequency for one given particle should decrease with increasing the amount of powder. We have indeed checked by varying the mass of powder by a factor of 2 that the time needed for full amorphization is proportional to the mass of powder all other milling parameters kept the same.

The specific milling intensity so defined has interesting properties: the higher the intensity, the larger the steady-state fraction of amorphous phase (Fig. 10). Full amorphization is obtained above a threshold specific milling intensity I_a^*. For the $Ni_{10}Zr_7$ compound at room temperature, $I_a^* = 510 \pm 30$ ms^{-2}.

B. Effect of milling temperature

Three runs (32, 33, 34) have been performed on the $Ni_{10}Zr_7$ compound at an average milling temperature of 200 °C. The following effects have been observed.

The threshold specific milling intensity, I_a^*, increases with the milling temperature. Full amorphization is achieved at room temperature with a milling intensity $I^* = 550$ ms^{-2}; at 200 °C, 90% amorphization is obtained at steady state with the same intensity (runs 6 and 33 in Table I).

Increasing the milling temperature slows down the amorphization kinetics and decreases the steady level of amorphization (Fig. 8). As an example, runs 32 and 4 are performed with the same milling intensity $I^* = 940$ ms^{-2} (above the amorphization threshold both at room temperature and at 200 °C). At 200 °C, full amorphization is only achieved after 190 h instead of 90 h at room temper-

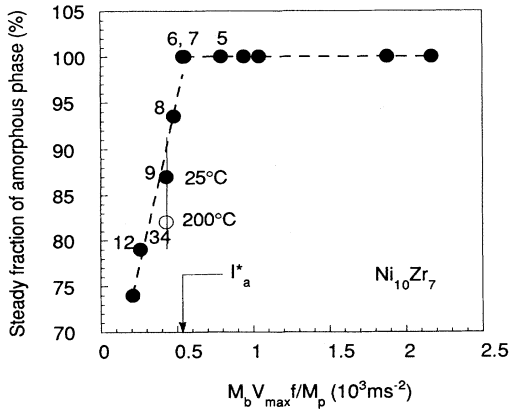

FIG. 10. Steady-state fraction of amorphous phase in $Ni_{10}Zr_7$ as a function of the specific milling intensity I_a^* is the intensity threshold for full amorphization.

ature. Runs 9 and 34 are performed below the amorphization threshold, at $I^*=430$ ms^{-2}: the steady amorphous fraction at 200 °C is about to 82% (run 34), to be compared to 86% reached at room temperature (run 9).

One experiment (35 in Table I) has been performed on $Ni_{10}Zr_7$ with a specific milling intensity $I^*=550$ ms^{-2}, up to 71 h, at −183 °C, circulating liquid N_2 around the vial. The amorphization kinetics at −183 °C and room temperature do not differ significantly.

C. Effect of alloy compositions

The amorphization threshold has been determined in many Ni-Zr alloys: the stœchiometric compounds Ni_5Zr, Ni_5Zr_2, $Ni_{10}Zr_7$, NiZr, $NiZr_2$ and two intermediate phases (54.4 and 63.5 at % Zr). To the exception of Ni_5Zr, all alloys could be fully amorphized above an appropriate threshold milling intensity. The x-ray-diffraction patterns of the amorphous phases are presented in Fig. 11. The Ni_5Zr alloy is too ductile: the powder transformed into a bulky layer sticking at the bottom of vial.

The amorphization threshold, I_a^*, depends on composition as shown in Fig. 12. As far as the stœchiometric compounds are concerned, I_a^* increases with the Zr content. Two-phase alloys exhibit a lower amorphization threshold I_a^* than that of the nearby stœchiometric compounds. As an example, $I_a^*=420\pm10$ ms^{-2} for the eutectic composition (63.5 at % Zr) as compared to 865 ± 70 ms^{-2} for NiZr and 1410 ± 470 ms^{-2} for $NiZr_2$.

D. Complementary experiments

In two distinct experiments, we checked that the same amorphous phase can be obtained by two different routes. Amorphous powders with $Ni_{10}Zr_7$ and $NiZr_2$ compositions, previously obtained by ball milling, have been introduced into the vial in such a proportion as to obtain an overall composition equal to $Ni_{50}Zr_{50}$. Milling was then performed for 80 h at room temperature and at a milling intensity above the amorphization threshold for

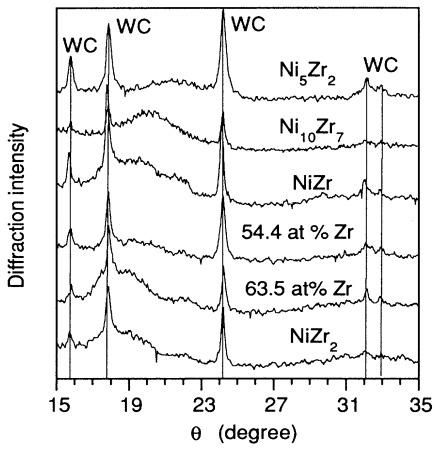

FIG. 11. X-ray-diffraction patterns of amorphized Ni_xZr_y alloys with six different compositions.

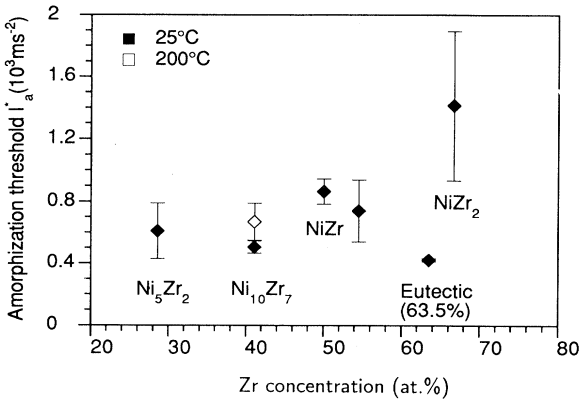

FIG. 12. Milling intensity threshold for full amorphization as a function of alloy composition.

the NiZr stœchiometric compound. The x-ray-diffraction pattern of the end product could not be distinguished from that of the NiZr compound amorphized directly. The amorphous alloy with eutectic composition can either be produced by milling a crystalline two-phase eutectic alloy or by milling a mixture of two crystalline stœchiometric compounds in the appropriate proportion.

IV. DISCUSSION

As we have seen, the milling conditions are characterized by a specific milling intensity, which is defined as the momentum transfer per unit time to the unit mass of powder, and by the overall milling temperature.

A. Effect of the specific milling intensity

As already discussed, the steady-state fraction of amorphous phase increases with increasing the milling intensity. In fact, the momentum transfer to the powder during an impact corresponds to the product of the impact force (F) and the duration of contact (δt): $F\delta t=M_b\delta V$. The energy transferred to the powder during the impact produces dry friction, welding, fracture, plastic shear in a way which cannot be evaluated quantitatively. Such processes nevertheless create topologic disorder (dislocations, grain boundaries, and antiphase boundaries) and chemical disorder (antisite defects); they also may create point defects in the crystalline phases and enhance atomic mobility by point-defect detrapping. The density of such defects should increase with the force and the duration of impact. The sensitivity of the end product to the impact frequency implies that some recovery process takes place between two impacts: dislocation rearrangements, antisite defects recovery by appropriate atomic jumps. Such process do not imply long-distance diffusion, but only local rearrangements on a few interatomic distances.

Amorphization results from a competition between the disordering of the crystalline structure and recovery processes. Jang and Koch[11] have already shown the existence of a dynamic equilibrium between the accumulation of defects and the restoration of the lattice during

high energy milling. The fact that an intermetallic compound transforms to an amorphous phase when it is sufficiently distorted has been established by several experimental works[12–14] and molecular-dynamics simulation studies: amorphization of several model intermetallic compounds ($NiZr_2$, Cu_xTi_y) can be obtained by simply accumulating antisite defects.[15–17]

B. Effect of the milling temperature

An effect of the overall milling temperature has been clearly identified in the present study. The amorphization kinetics is slower and the steady-state proportion of the amorphous phase is lower, the higher the temperature. Compared to room-temperature experiments, large effects are observed on increasing the temperature up to 200 °C, while no noticeable effect is found on decreasing the latter to −183 °C. We therefore safely conclude that the effect of the milling temperature is not related to the quenching rate of the thermal spike which is expected to be produced by the impact. In our grinder, the maximum local temperature rise is estimated below 10 K for all milling conditions used.[18]

Similar milling temperature effects have already been reported by Gaffet and Yousfi.[6] In the planetary mill they used at four temperatures (25, 100, 200, and 300 °C), the higher the temperature, the narrower the parameter window for full amorphization: the latter cannot be obtained at 300 °C and above.

In order to clarify the effect of the milling temperature, amorphous $Ni_{10}Zr_7$ powder has been annealed at 200 °C up to 100 h. Typical x-ray-diffraction patterns after 1, 20, and 100 h annealing are shown in Fig. 13. No crystallization is observed up to 100 h. Nevertheless, the impact frequency effect which has been identified in the previous section implies a competition between some sort of disordering and annealing. The latter cannot be the recrystallization of the amorphous phase. We suggest the competition occurs, inside the crystalline structure, between the disorder induced by collisions and thermally activated recovery.

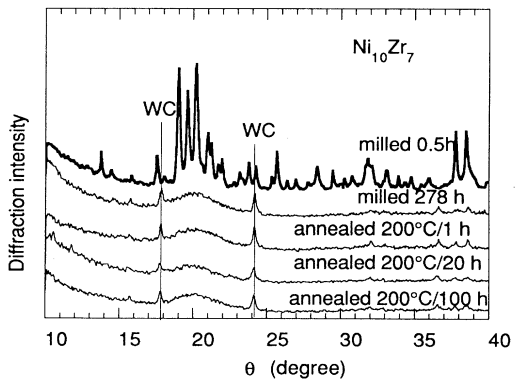

FIG. 13. X-ray-diffraction patterns of $Ni_{10}Zr_7$ amorphous powders annealed at 200 °C for 1, 20, and 100 h. The spectra of the unannealed amorphous powder and of the crystalline powder are given as a reference.

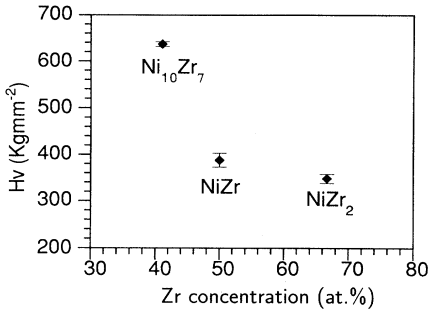

FIG. 14. Microhardness for three intermetallic compounds: $Ni_{10}Zr_7$, NiZr, $NiZr_2$ (Ref. 19).

C. Effect of alloy composition

The room-temperature milling intensity threshold for full amorphization of the three intermetallic compounds $NiZr_2$, NiZr, and $Ni_{10}Zr_7$ varies as $I_a^*(NiZr_2) > I_a^*(NiZr) > I_a^*(Ni_{10}Zr_7)$. It is worth noticing that this correlates inversely with their Vickers hardness:[19] $Hv(NiZr_2) < Hv(NiZr) < Hv(Ni_{10}Zr_7)$ (Fig. 14). The harder the compound, the easier the amorphization. A Ni_5Zr compound could not be amorphized because of its high ductility. The higher the hardness, the more brittle the compound, and the more frequent the fracture-welding events which we believe are at the origin of chemical mixing which promotes amorphization.

Finally, we have shown that the same amorphous alloy ($Ni_{50}Zr_{50}$) can be obtained in the same milling device by two distinct routes: the first one implying an increase, the second one a decrease of internal (or free) energy. Internal energy arguments are therefore difficult to accept as a basis for rationalizing the effects of ball milling. The mechanical and elastic properties of competing phases as well as their chemical stability must enter the criterion for phase stability under high-energy milling.

V. CONCLUSION

We have demonstrated that the respective stability of the amorphous and crystalline forms of Ni_xZr_y compounds under ball milling cannot be assessed from simple energy arguments but can be rationalized in terms of a composition and temperature-dependent specific milling intensity, defined as the momentum transferred per unit time to the unit mass of powder. The latter controls the rate of amorphization and the steady-state fraction of phases in two-phase equilibria. The mechanism of amorphization by ball milling is worth studying in more detail.

ACKNOWLEDGMENTS

The assistance of Dr. L. Boulanger for electron microscopy and of M. Sapin for x-ray diffraction is gratefully acknowledged.

APPENDIX

The frame performs a sinusoidal vertical movement with amplitude A ($\approx$ mm) and pulsation ω (100π s^{-1}). The altitude of the vial in the laboratory at time t is $Y = A\sin\omega t$. In the case of a fully plastic collision between the ball and the powder in the vial, the ball comes to rest with respect to the vial after each collision. Assuming no dry friction between the ball and the powder during the next takeoff, the launching condition writes

$$A\omega^2 \sin\omega t \geq g \ ,$$

where g is the gravitational acceleration. The takeoff velocity of the ball in the laboratory is

$$V_1 = \sqrt{A^2\omega^2 - g^2/\omega^2}$$
$$\approx \omega A = V_{\max}$$

since it is easily checked that $A\omega^2 \gg g$.

The velocity of the ball relative to the vial at time of impact can be determined exactly solving the equations of movement. The movement of the ball is strictly periodic.

However, because of irregularities either in the movement of the frame or in the restitution coefficient (now and then, the ball lands on a large hard grain of powder) the ball deviates from a vertical trajectory and some randomness is introduced in the movement of the ball. As a first guess, the velocity of the ball relative to the vial can be averaged over a large number of collisions, as follows. Assuming the collisions occur at any time in a vibration cycle, the average relative velocity writes

$$\langle V_b - V \rangle = \frac{\omega}{2\pi} \int_{-\pi/\omega}^{\pi/\omega} [V_b(t') - V(t')]dt'$$
$$= \frac{\omega}{2\pi} \int_{-\pi/\omega}^{\pi/\omega} [V_{\max} - gt' - A\omega\cos(\omega t')]dt'$$
$$= V_{\max}$$

since $g \ll A\omega^2/\pi$. The average momentum transfer from the ball to the powder, $M_b\langle V_b - V \rangle$, is thus of the order of $M_b V_{\max}$.

[1](a) A. W. Weeber, A. J. H. Wester, W. J. Haag, and H. Bakker, Physica B **145**, 349 (1987); (b) J. Eckert, L. Schultz, and E. Hellstern, J. Appl. Phys. **64**, 3224 (1988).

[2]R. B. Schwarz and R. R. Petrich, J. Non Cryst. Solids **76**, 281 (1985).

[3]G. Martin and P. Bellon, J. Less Common Met. **140**, 211 (1988).

[4]F. Haider, P. Bellon, and G. Martin, Phys. Rev. B **42**, 8274 (1990).

[5]G. Martin and E. Gaffet, J. Phys. (Paris) Colloq. **51**, C4-71 (1990).

[6]E. Gaffet and L. Yousfi, Proceedings of the International Symposium on Mechanical Alloying, Kyoto, Japan [Mater. Sci. Forum **88-90**, 51 (1991)].

[7]J. Eckert, L. Schultz, and K. Urban, J. Mater. Sci. **26**, 441 (1991).

[8]Y. Chen (unpublished).

[9]A. Mehta and J. M. Luck, Phys. Rev. Lett. **65**, 393 (1990).

[10]A. Antoniadis, J. Berruyer, and A. Filhol (unpublished).

[11]J. S. C. Jang and C. C. Koch, J. Mater. Res. **5**, 498 (1990).

[12]Y. Seki and W. L. Johnson, in *Solid State Powder Processing*, edited by A. H. Clauer and J. J. deBarbadillo (TMS, Warrendale, 1990), p. 287.

[13]H. Bakker, L. M. Di, and D. M. R. L. Cascio, Proceeding of the International Symposium on Mechanical Alloying, Kyoto, Japan [Mater. Sci. Forum **88-90**, 27 (1991)].

[14]L. E. Rehn, P. R. Okamoto, J. Pearson, R. Bhadra, and M. Grimsditch, Phys. Rev. Lett. **59**, 2987 (1987).

[15]N. Q. Lam, P. R. Okamoto, R. Devanathan, and M. Meshii, *Statics and Dynamics of Alloy Phase Transformations*, NATO Advanced Study Institute (Plenum, New York, in press).

[16]C. Massobrio, V. Pontikis, and G. Martin, Phys. Rev. B **41**, 10486 (1990).

[17]Y. Limoge and A. Rahman, J. Non Cryst. Solids **99**, 75 (1988).

[18]Y. Chen, R. Le Hazif, and G. Martin, in *Non Linear Phenomena in Materials Science II*, edited by G. Martin and L. Kubin [Solid State Phenomena **23-24**, 271 (1992)].

[19]D. Galy (unpublished).

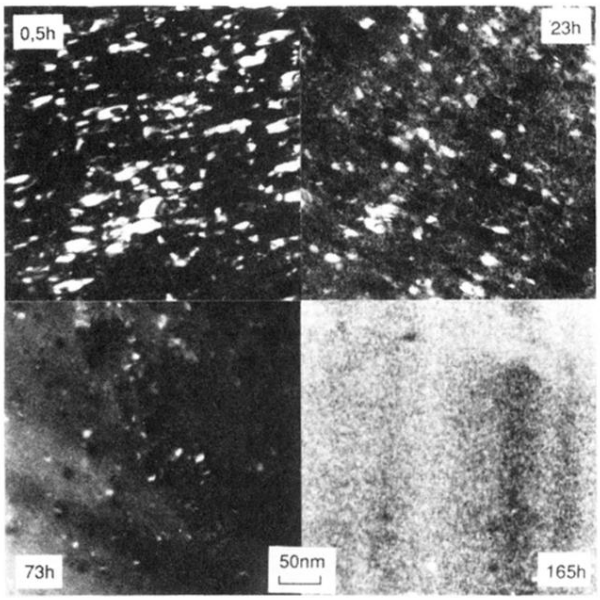

FIG. 4. Dark-field TEM micrographs of $Ni_{10}Zr_7$ milled for 0.5, 23, 73, and 165 h at room temperature with a ball mass of 0.5 kg and a vibration amplitude of 1.5 mm.

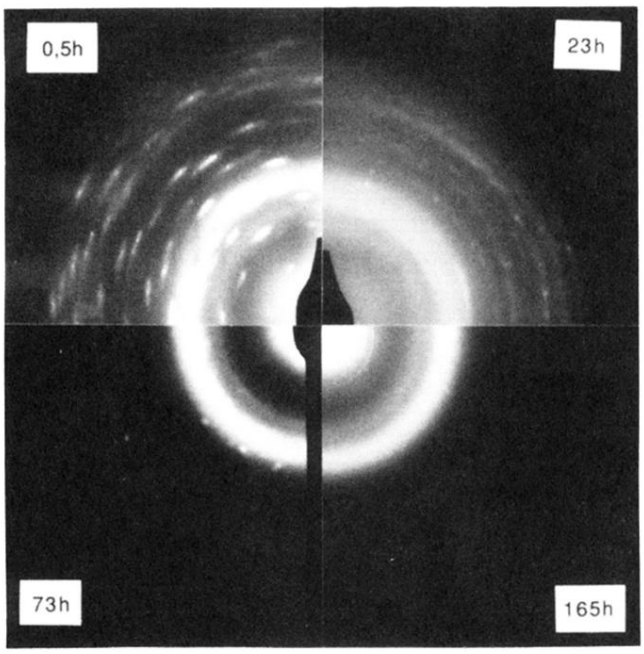

FIG. 5. Corresponding electron-diffraction patterns.

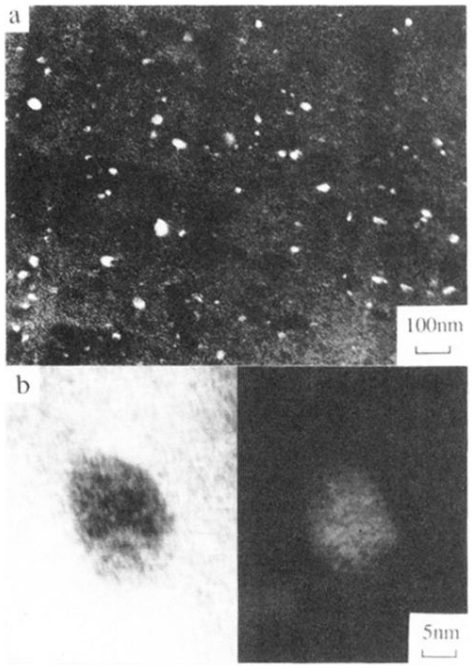

FIG. 7. (a) Dark-field micrograph of $Ni_{10}Zr_7$ milled for 370 h with a ball mass of 300 g and a vibration amplitude of 1.0 mm. (b) High magnification bright and dark-field images of a nanometer size crystallite surrounded by the amorphous phase. Notice the high quality of the crystalline phase where the lattice planes seem undistorted.